

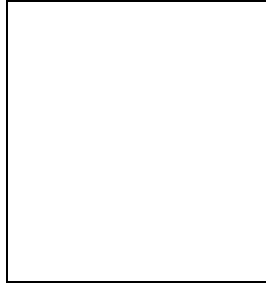
New results on nuclear dependence of J/ψ and ψ' production in 450 GeV pA collisions

R. SHAHOYAN for NA50 Collaboration

M.C. Abreu^{6,a}, B. Alessandro¹⁰, C. Alexa³, R. Arnaldi¹⁰, M. Atayan¹², C. Baglin¹, A. Baldit², M. Bedjidian¹¹, S. Beolè¹⁰, V. Boldea³, P. Bordalo^{6,b}, S.R. Borenstein^{9,c}, G. Borges⁶, A. Bussière¹, L. Capelli¹¹, C. Castanier², J. Castor², B. Chaurand⁹, B. Cheynis¹¹, E. Chiavassa¹⁰, C. Cicalò⁴, T. Claudino⁶, M.P. Comets⁸, N. Constans⁹, S. Constantinescu³, P. Cortese^{10,d}, J. Cruz,⁶, N. De Marco¹⁰, A. De Falco⁴, G. Dellacasa^{10,d}, A. Devaux², S. Dita³, O. Drapier¹¹, B. Espagnon², J. Fargeix², P. Force², M. Gallio¹⁰, Y.K. Gavrilov⁷, C. Gerschel⁸, P. Giubellino¹⁰, M.B. Golubeva⁷, M. Gomin⁹, A.A. Grigorian¹², S. Grigorian¹², J.Y. Grossiord¹¹, F.F. Guber⁷, A. Guichard¹¹, H. Gulkanyan¹², R. Hakobyan¹², R. Haroutunian¹¹, M. Idzik^{10,e}, D. Jouan⁸, T.L. Karavitcheva⁷, L. Kluberg⁹, A.B. Kurepin⁷, Y. Le Borne^c, C. Lourenço⁵, P. Macciotta⁴, M. Mac Cormick⁸, A. Marzari-Chiesa¹⁰, M. Masera¹⁰, A. Masoni⁴, M. Monteno¹⁰, A. Musso¹⁰, P. Petiau⁹, A. Piccotti¹⁰, J.R. Pizzi¹¹, W. Prado da Silva^{10,f}, F. Prino¹⁰, G. Puddu⁴, C. Quintans⁶, S. Ramos^{6,b}, L. Ramello^{10,d}, P. Rato Mendes⁶, L. Riccati¹⁰, A. Romana⁹, H. Santos⁶, P. Saturnini², E. Scalas^{10,d}, E. Scomparin¹⁰, S. Serci⁴, R. Shahoyan^{6,g}, F. Sigaudo¹⁰, S. Silva⁶, M. Sitta^{10,d}, P. Sonderegger^{5,b}, X. Tarrago⁸, N.S. Topilskaya⁷, G.L. Usai⁴, E. Vercellin¹⁰, L. Villatte⁸, N. Willis⁸.

¹ LAPP, CNRS-IN2P3, Annecy-le-Vieux, France. ² LPC, Univ. Blaise Pascal and CNRS-IN2P3, Aubière, France. ³ IFA, Bucharest, Romania. ⁴ Università di Cagliari/INFN, Cagliari, Italy. ⁵ CERN, Geneva, Switzerland. ⁶ LIP, Lisbon, Portugal. ⁷ INR, Moscow, Russia. ⁸ IPN, Univ. de Paris-Sud and CNRS-IN2P3, Orsay, France. ⁹ LPNHE, Ecole Polytechnique and CNRS-IN2P3, Palaiseau, France. ¹⁰ Università di Torino/INFN, Torino, Italy. ¹¹ IPN, Univ. Claude Bernard Lyon-I and CNRS-IN2P3, Villeurbanne, France. ¹² YerPhI, Yerevan, Armenia.

a) also at UCEH, Universidade de Algarve, Faro, Portugal b) also at IST, Universidade Técnica de Lisboa, Lisbon, Portugal c) on leave of absence from York College CUNY d) Università del Piemonte Orientale, Alessandria and INFN-Torino, Italy e) also at Faculty of Physics and Nuclear Techniques, University of Mining and Metallurgy, Cracow, Poland f) now at UERJ, Rio de Janeiro, Brazil g) on leave of absence from YerPhI, Yerevan, Armenia



To understand the reliability of the charmonia suppression as a signature of the Quark-Gluon Plasma formation in nucleus-nucleus collisions it is important first to understand the details of the production of J/ψ and ψ' in pA interactions and the difference in the suppression of these two states. This report presents the results of the study by the NA50 collaboration of the J/ψ and ψ' production in pA interactions at 450 GeV beam energy and its dependence on rapidity. It is shown that the ψ' suffers more suppression than the J/ψ , which is consistent with a similar observation made at 800 GeV beam energy by the E866/NuSea collaboration.

1 Introduction

The suppression of the production of charmonia states (mainly J/ψ and ψ') in $nucleus-nucleus$ interactions due to colour screening is recognized as one of the most promising QGP signatures¹. But in real experiments it should be distinguished from the suppression due to the hadronic interactions of charmonia with surrounding nuclear matter. This kind of suppression, present already in pA interactions, can describe all currently available data except the “anomalous J/ψ suppression” observed by the NA50 experiment in PbPb collisions². The deconvolution of these two kinds of suppression requires precise quantitative understanding of the interaction of different charmonium states with hadronic matter. While a vast amount of data was collected for the J/ψ , the situation with the ψ' is less clear. Published NA50 data showed similar levels of suppression for both mesons in pA collisions but a stronger suppression of the ψ' in heavier colliding systems, like SU³, which was attributed to additional absorption of the ψ' due to interactions with “comovers” - hadrons produced in the collision. Finally, the E866/NuSea collaboration⁴ observed a stronger suppression for the ψ' already in 800 GeV pA interactions. The motivation of the present study is to look for similar effects in the NA50 data.

2 Experimental setup, data samples and analysis

The main component of the NA50 apparatus is a dimuon spectrometer, covering the $3.0 < y_{lab} < 4.0$ rapidity range, which is separated from the target region by a 4.8 m long hadron absorber. The dimuon trigger is provided by four scintillator hodoscopes and its efficiency is controlled during special runs by two additional hodoscopes. The detailed description of the experiment can be found in⁵. We present here the analysis of data collected in the 1996-2000 period with a 450 GeV proton beam interacting with Be, Al, Cu, Ag and W targets. Each data sample was obtained with single target, with interaction probability varying from 26 (Al) to 39 (Ag)%. The incoming beam intensity was monitored by three argon ionization chambers. For each target two qualitatively different data samples were collected: with “low” (**LI**, $1 - 3 \times 10^8$ protons per 2.37 s spill) and “high” (**HI**, $1 - 3 \times 10^9$ p/spill) beam intensities. While the **LI** samples^a are more reliable from the absolute normalization point of view, the **HI** one provides much better statistics, which is necessary for the ψ' study.

The reconstructed dimuons were subjected to $-0.5 < y_{cm} < 0.5$ and $|\cos \theta_{CS}| < 0.5$ selection cuts. For the differential cross section studies, the rapidity range was divided in four equidistant bins. The mass spectra in each kinematical bin were fitted with curves corresponding to individual dimuon sources, obtained from detailed Monte-Carlo simulations.

Combinatorial background from uncorrelated $\pi, K \rightarrow \mu$ decays was estimated from the like-sign dimuon samples (using the relation $N_{+-} = 2R\sqrt{N_{++}N_{--}}$, with R being a free parameter of the fit, accounting for possible charge correlations in parent hadrons production). The contribution from the dimuons originated in interactions outside of the target was accounted by including into the fit the dimuon spectrum obtained from the special “target-out” runs.

The systematic errors of the extracted cross sections account for uncertainties in the normalization: luminosity, trigger and reconstruction efficiencies.

Since various authors use different parametrizations for the description of charmonia suppression, we fitted the obtained cross sections by three commonly used models:

- 1) The Glauber model, assuming that each charmonium state i is produced in binary nucleon-nucleon interactions with cross section σ_0^i and then interacts with surrounding nuclear matter with cross section σ_{abs}^i . This leads to the pA cross section $\sigma_{pA} = \sigma_0/\sigma_{abs}^2 \int d\vec{s} [1 - T_A(\vec{s})\sigma_{abs}]^A$, where $T_A(\vec{s})$ is the nuclear thickness function at impact vector \vec{s} .
- 2) A simplification of the Glauber model, assuming that the charmonium is absorbed with cross

^aThe results for the **LI** sample were presented in⁶ (obtained with a somewhat different analysis procedure).

section σ_0 seeing in average $\langle \rho L \rangle$ amount of matter from its production point to its exit from the nucleus: $\sigma_{pA} = \sigma_0 A e^{-\sigma_{abs} \langle \rho L \rangle}$ ($\langle \rho L \rangle = (A-1)/2 \int d\vec{s} T_A^2(\vec{s})$ is obtained from the expansion of the Glauber formula).

3) The widely used although not theory-motivated parametrization $\sigma_{pA} = \sigma_0 A^\alpha$.

3 Results

Table 1 shows the J/ψ and ψ' cross sections in the whole rapidity range (first column) and in four separate bins (columns 2-5). Due to the lack of space we show the cross sections obtained from the **HI** data sample only. Although the cross sections extracted from the **LI** data sample are systematically higher, it is the same $\sim 5\%$ difference both for the J/ψ and the ψ' , which justifies the treatment of this discrepancy as a constant normalization factor. One should notice that since the systematic errors reflect the uncertainty in the absolute normalizations, they do not affect the shapes of the differential distributions in rapidity.

Table 1: J/ψ and ψ' cross sections per nucleon in nb (not corrected for the $\mu\mu$ branching ratio) for the integrated data and in four Y_{CM} bins. The statistical and systematic errors are shown separately.

	$-0.50 < Y < 0.50$	$-0.50 < Y < -0.25$	$-0.25 < Y < 0.0$	$0.0 < Y < 0.25$	$0.25 < Y < 0.5$
J/ψ					
pBe	$5.130 \pm 0.010 \pm 0.177$	$1.202 \pm 0.007 \pm 0.042$	$1.373 \pm 0.004 \pm 0.047$	$1.352 \pm 0.004 \pm 0.047$	$1.210 \pm 0.007 \pm 0.042$
pAl	$4.868 \pm 0.008 \pm 0.228$	$1.117 \pm 0.005 \pm 0.053$	$1.304 \pm 0.003 \pm 0.061$	$1.281 \pm 0.003 \pm 0.060$	$1.145 \pm 0.005 \pm 0.054$
pCu	$4.712 \pm 0.006 \pm 0.181$	$1.173 \pm 0.004 \pm 0.045$	$1.275 \pm 0.003 \pm 0.049$	$1.209 \pm 0.003 \pm 0.047$	$1.069 \pm 0.004 \pm 0.041$
pAg	$4.403 \pm 0.005 \pm 0.148$	$1.077 \pm 0.004 \pm 0.036$	$1.190 \pm 0.002 \pm 0.040$	$1.134 \pm 0.002 \pm 0.038$	$1.016 \pm 0.004 \pm 0.034$
pW	$4.005 \pm 0.006 \pm 0.147$	$0.945 \pm 0.004 \pm 0.035$	$1.068 \pm 0.003 \pm 0.039$	$1.047 \pm 0.003 \pm 0.038$	$0.945 \pm 0.004 \pm 0.035$
ψ'					
pBe	$.0886 \pm .0021 \pm .0032$	$.0207 \pm .0014 \pm .0008$	$.0231 \pm .0010 \pm .0008$	$.0228 \pm .0009 \pm .0008$	$.0217 \pm .0013 \pm .0009$
pAl	$.0841 \pm .0015 \pm .0044$	$.0194 \pm .0010 \pm .0009$	$.0215 \pm .0006 \pm .0011$	$.0228 \pm .0006 \pm .0012$	$.0209 \pm .0009 \pm .0010$
pCu	$.0773 \pm .0011 \pm .0032$	$.0189 \pm .0007 \pm .0008$	$.0210 \pm .0005 \pm .0008$	$.0197 \pm .0004 \pm .0009$	$.0173 \pm .0007 \pm .0009$
pAg	$.0690 \pm .0010 \pm .0025$	$.0151 \pm .0006 \pm .0005$	$.0189 \pm .0004 \pm .0007$	$.0182 \pm .0004 \pm .0007$	$.0161 \pm .0006 \pm .0005$
pW	$.0611 \pm .0010 \pm .0024$	$.0130 \pm .0006 \pm .0005$	$.0161 \pm .0004 \pm .0006$	$.0162 \pm .0004 \pm .0007$	$.0158 \pm .0007 \pm .0006$

Fig. 1 shows the J/ψ and ψ' absorption parameters obtained from the global fit of **HI** and **LI** data samples by the models mentioned in Sec.2. For these joint fits the cross sections from the **HI** and **LI** samples were rescaled by the factors $2/(1+R)$ and $2R/(1+R)$, respectively ($R = 0.957$ is the result of the fit of the ratio of **HI** to **LI** values by a constant line). The results obtained separately from **HI** and **LI** samples are similar to the shown results. The large symbols in the center correspond to the fit of the data integrated over the $-0.5 < y_{cm} < 0.5$ range.

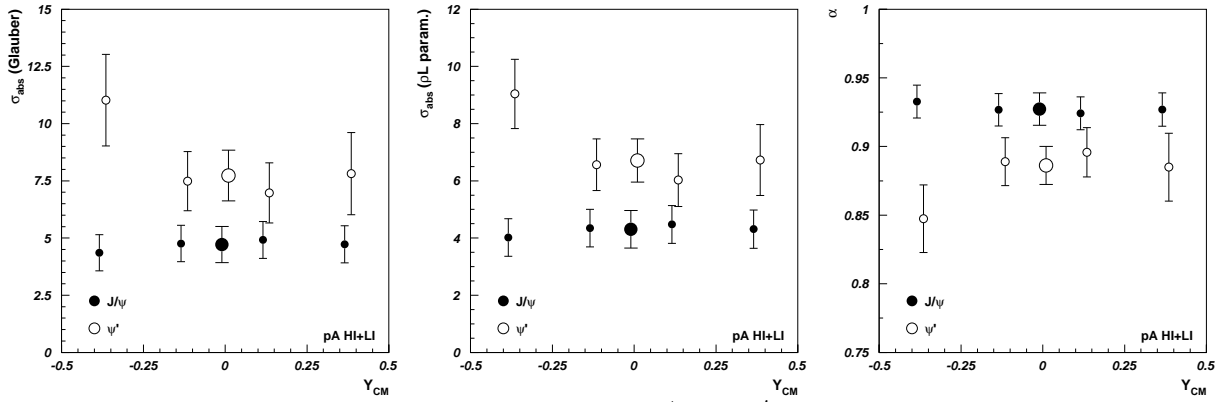


Figure 1: α parameters and absorption cross sections for the J/ψ and ψ' as a function of the Y_{CM} obtained from the absolute cross sections fit: (Left) Glauber model; (Center) $e^{-<\rho L> \sigma_{abs}}$; (Right) A^α parametrizations. The large symbols in the center correspond to fitting the data integrated over $-0.5 < y_{cm} < 0.5$.

Finally, Fig. 2 shows the difference between the α parameters and σ_{abs} of the J/ψ and ψ' states extracted from fitting directly the ψ' to J/ψ cross section ratio (which cancels the uncertainties in the normalization). The full Glauber model is not applicable to cross sections ratios, so we show only the results of the $e^{-<\rho L>\sigma_{abs}}$ parametrization.

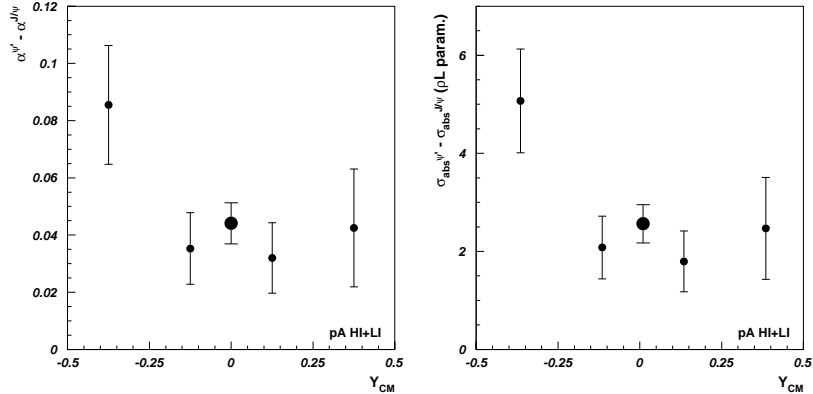


Figure 2: Difference in the α parameters (Left) and in the absorption cross sections from the $e^{-<\rho L>\sigma_{abs}}$ parametrization for the J/ψ and ψ' states as a function of Y_{CM} . Obtained from the direct fit of the ψ' to J/ψ cross sections ratio.

4 Summary

The production cross sections of J/ψ and ψ' in 450 GeV pA interactions was obtained and analyzed in the framework of charmonia nuclear absorption models. The J/ψ nuclear absorption in the $-0.5 < y_{cm} < 0.5$ range is consistent with previous NA50 results and yields $\alpha_{J/\psi}^{J/\psi} = 0.927 \pm 0.012$ (for $\sigma_{pA} = \sigma_0 A^\alpha$ parametrization). The fit with the full Glauber model yields $\sigma_{abs}^{J/\psi} = 4.7 \pm 0.8$ mb (or 4.3 ± 0.7 mb for the $e^{-<\rho L>\sigma_{abs}}$ parametrization). The corresponding fits for the ψ' show a stronger absorption than for the J/ψ , thus confirming the results of the E866 collaboration: $\alpha_{\psi'}^{J/\psi} = 0.886 \pm 0.014$ (with $\sigma_{abs}^{\psi'} = 7.7 \pm 0.8$ and 6.7 ± 0.8 mb for the Glauber and the $e^{-<\rho L>\sigma_{abs}}$ models respectively). The more precise fit of the ratio of ψ' to J/ψ cross sections yields $\alpha_{J/\psi}^{J/\psi} - \alpha_{\psi'}^{J/\psi} = 0.045 \pm 0.007$ and $\sigma_{abs}^{\psi'} - \sigma_{abs}^{J/\psi} = 2.6 \pm 0.4$ nb (for the $e^{-<\rho L>\sigma_{abs}}$ parametrization). No statistically significant dependence of the absorption on the rapidity is seen, although there is an indication of a stronger absorption of the ψ' at small rapidities.

Acknowledgments

The work was supported by the Fundação para a Ciência e a Tecnologia under the contract RPAXIS XXI/BD/16116/98. I appreciate the support of LIP in attending this conference.

References

1. T.Matsui and H.Satz, Phys. Lett. **B178** (1986) 416.
2. M.C.Abreu *et al.* (NA50 Collaboration), Phys.Lett **B477** (2000) 28.
3. L. Ramello *et al.* (NA50 Collaboration), Nucl.Phys. **A638** (1998) 261.
4. M.J.Leitch *et al.* (E866/NuSea Collaboration), Phys.Rev.Lett. **84** (2000) 3256.
5. M.C. Abreu *et al.* (NA50 Collaboration), Nucl. Phys. **B410** (1997) 327.
6. E. Scomparin *et al.* (NA50 Collaboration), Nucl. Phys. **A698** (2002) 543c.